Journal of the Australian Ceramic Society (2022) 58:63–70
https://doi.org/10.1007/s41779-021-00656-4

RESEARCH

New cobalt phthalocyanine–graphene oxide hybrid nanomaterial prepared by strong π–π interactions

Ebru Yabaş[1]

Received: 11 July 2021 / Revised: 22 August 2021 / Accepted: 11 September 2021 / Published online: 4 October 2021

Abstract

In this study, a novel hybrid nanomaterial was obtained by interaction of cobalt phthalocyanine (CoPc) derivative on the surface of graphene oxide (GO) producing a CoPc-GO supermolecular system in which interaction is occurred by the π–π stacking. The CoPc-GO hybrid was prepared in a much shorter time than the examples in the literature, and it was observed that this nanomaterial was quite stable at room conditions and during dilution. The obtained hybrid nanomaterial was analyzed by scanning electron microscopy (SEM) and spectroscopic methods. Spectroscopic measurements indicate that immediate intermolecular interactions are occurring during the mixing of GO and CoPc. SEM studies show that CoPc successfully interacts with GO. Significant color changes were also observed by the addition of GO solutions at different concentrations on the CoPc solution. Also, we determined the optical band gap of the CoPc-GO nanohybrid using UV–Vis spectroscopy technique. It was also determined that the stable CoPc-GO hybrid, which can be prepared very quickly and easily, has the potential to be used in optoelectronic applications.

Keywords Phthalocyanine · Graphene oxide · Synthesis · Hybrid · Nanomaterial

Introduction

GO has an extremely high surface area, is easy to prepare, and has very good biocompatibility and long-term biodistribution. Because of these properties, GO may interact with various biomolecules for drug delivery and gene transfection applications [1–4]. On the other hand, GO structure comprises various oxygen-containing functional groups. The oxygen functional groups have been identified as most in the form of hydroxyl and epoxy groups on the basal plane, with smaller amounts of carboxyl, phenol, lactone, and quinone at the sheet edges [5–7]. The presence of such types of functional groups can ensure potential advantages for using GO in numerous other applications. This is dedicated to the fact that the polar oxygen-containing functional groups make GO strongly hydrophilic, according to which it can disperse significantly well in many polar solvents, particularly in water [8–11]. This ability of GO is very important for processing and further derivatization of it because the obtained stable dispersion of GO can be subsequently deposited on various surfaces to prepare for example thin conductive films that can be used as excellent electrode materials [7]. Another positive side of the presence of oxygen-containing functional groups in the structure of GO is that it is possible to use them as sites for chemical modification or functionalization of GO through covalent or non-covalent bonds using well-known chemistry strategies for the design of various sensitive hybrid systems with extraordinary exceptional properties [5]. Indeed, obtained hybrid compounds possess a broad spectrum of various properties, which allow using them as catalysts [12], photoelectrodes [13], electrochemical sensors [14], components for enhancement of lithium storage capacity [15] and with lower charge-transfer resistance [16], etc. Such unusual properties emerge by functionalization of GO with nanoparticles [17–20], quantum dots [13, 21–23], various classes of organic compounds [24–26], polymers [27–29], and particularly biomolecules [30–32]. Until now, a wide range of organic compounds, such as porphyrins [33–35], aromatic dyes [16], alkylamines [24], ionic liquids [36], pyrene derivatives [25], cyclodextrin [26], and aryl diazonium compounds [37] have been noncovalently or covalently attached onto the GO nanosheets to generate functional organic nanocomposites for various applications.

✉ Ebru Yabaş
eyabas@cumhuriyet.edu.tr

[1] Advanced Technology Application and Research Center, Sivas Cumhuriyet University, 58140 Sivas, Turkey

Among these classes of compounds, GO is also modified with metal phthalocyanine for having unique physicochemical properties with outstanding electronic and optical properties to utilize them in medicine, electrochemistry etc.

Considering the importance of GO modified phthalocyanine, in this study, I have prepared and characterized CoPc-GO hybrid nanomaterial. Although previous reports suggest that prolonged sonication at elevated temperatures is necessary for the modification of GO with phthalocyanine, this work shows that the attachment could in fact be completed rapidly and at ambient temperatures by appropriate designing of the CoPc. To the best of our knowledge, this is the first report showing that strong π–π interactions between CoPc and GO components can occur in as little as 5 min by sonication.

Experimental

Materials and equipment

CoPc was prepared according to the literature [38]. The absorption and fluorescence spectra were recorded by a Shimadzu UV-1800 spectrophotometer and Agilent Cary Eclipse G9800A Fluorescence Spectrometer, respectively. The surface morphology of CoPc-GO was observed by using a TESCAN MIRA3 XMU SEM. Sonics VCX-750 Vibra Cell was used for the sonication process. GO and CoPc-GO hybrid solutions were prepared in a sonicator. Optical characterization was carried out using Cary 5000 UV–Vis-NIR spectrophotometer.

Synthesis of CoPc

The detailed synthesis route is given in our previous study [38]. The synthesis steps were as follows: ın the first step, 4-[(4′-(Tert-butyl)phenoxy)phenoxy]phthalonitrile has been synthesized by the reaction of 4-(4-nitrophenoxy)phthalonitrile with 4-tertiarylbutylphenole. In the second step, CoPc was prepared by tetramerization reaction of synthesized 4-[(4′-(Tert-butyl)phenoxy)phenoxy]phthalonitrile in the presence of $CoCl_2$.

Synthesis of CoPc-GO hybrid

GO solutions (0.00005 µg/mL; 0.0005 µg/mL; 0.005 µg/mL; 0.05 µg/mL; 0.4 µg/mL; 0.7 µg/mL; 1 µg/mL) were prepared by sonication in DMSO. The solution of 10 µg/mL of CoPc in DMSO (5 mL) was added to different concentrations of GO solution (5 mL), respectively. The prepared solutions were sonicated for 5 min.

Preparation of thin film

To prepare thin film, CoPc-GO hybrid in powder form was dispersed in THF. Then, the prepared solution was dropped onto glass surfaces and dried at room temperature.

Results and discussion

The schematic interaction process of CoPc and GO is shown in Fig. 1. GO lattices having sufficient electron delocalization function as suitable adsorption sites for CoPc. GO represents an extensive delocalized π–electron planar system, which promotes interaction with CoPc through π–π stacking interaction. Since the molecules of phthalocyanine can aggregate at high concentrations [39], a dilute solution of CoPc (10 µg/mL) was used, which will also provide adequate interaction between molecules of GO and CoPc.

Subsequently, various concentrations of GO in DMSO were prepared, mixed with CoPc in DMSO solution by sonication and the resultant solutions were studied by UV–Vis and fluorescence spectroscopy. The absorption spectra of CoPc in DMSO after the addition of GO with various concentrations are shown in Fig. 2.

As can be seen from the spectra, increasing GO concentration leads to the decrease in peak intensity and shifts from 672 nm (GO concentration is 0) to 695 nm (GO concentration is 1 µg/mL). Considering this alteration, we can say that strong π–π interaction occurs between GO and CoPc with increasing GO concentration. This effect is observed by flattening of the curves in Fig. 2B. Due to the presence of keen π–π interactions, the molecules of CoPc are densely adsorbed on the lattices of GO producing CoPc-GO hybrid. With the formation of CoPc-GO hybrid, a redshift of 23 nm was observed in the UV–Vis spectra. This shift shows us that this material may have the potential to be used in optoelectronic applications.

The fluorescence spectra of the above samples are shown in Fig. 3. As can be seen from the fluorescence spectra, increasing GO concentration leads to the gradual decline of the emission intensity, which demonstrates effective electron transfer from CoPc to GO. According to the literature [40], organic dyes with H-aggregates are not fluorescent. Considering the effective fluorescence emission quenching, we can say that CoPc-GO hybrid system may be used in optoelectronics as the active material. Spectroscopic measurements show that hybrid formation is complete when CoPc concentration is 10 µg/mL and GO concentration is 1 µg/mL. Accordingly, it can be said that the mass ratio in the CoPc-GO hybrid formation is about 1:10.

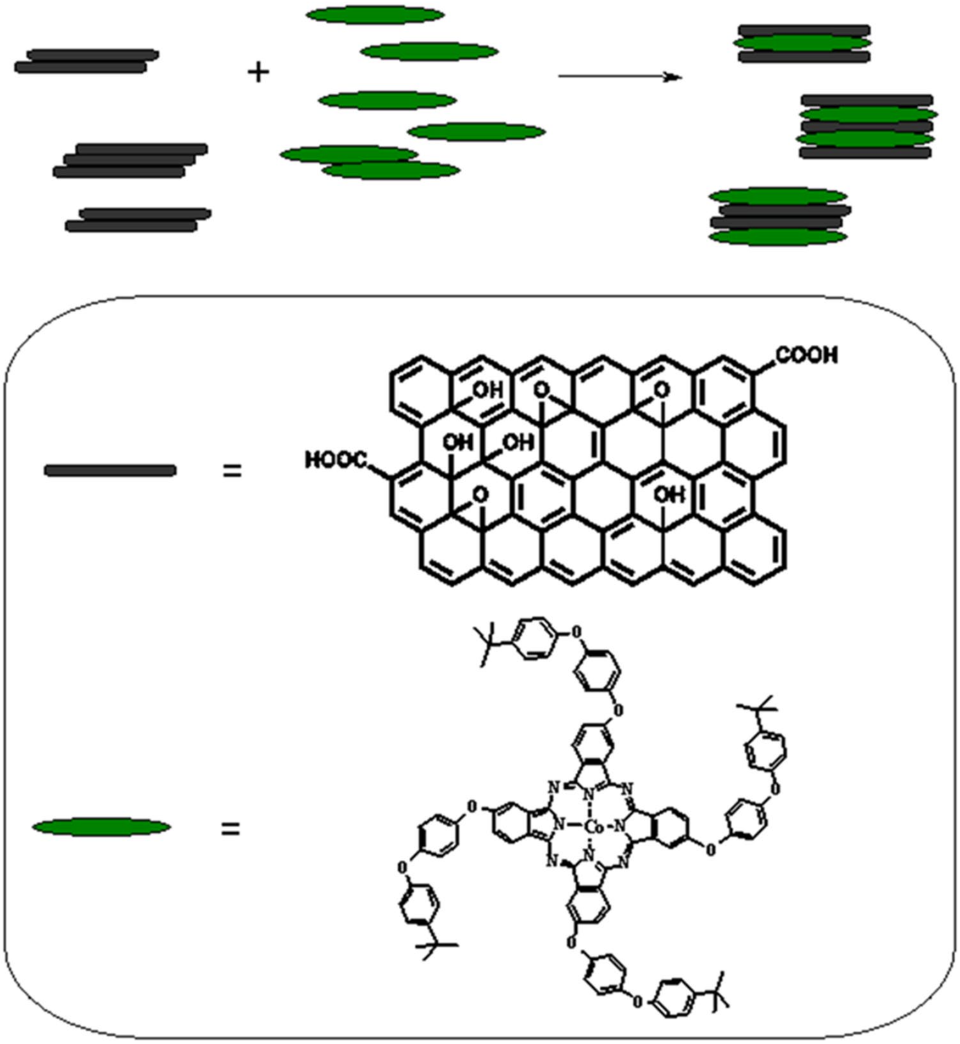

Fig. 1 Illustration showing the formation of CoPc-GO hybrid

As shown in Fig. 4, as the concentration of GO added on CoPc increases, significant color changes are observed in the solutions. As described above, color changes are noticeable in parallel with spectroscopic changes due to GO concentration. Furthermore, it is also easy to determine that the CoPc-GO hybrid formation is complemented by this color change.

Figure 5 shows the SEM images of CoPc-GO nanomaterial hybrids prepared separately by adding different concentrations of GO solution (0.0005 µg/mL, 0.005 µg/mL, 0.4 µg/mL, 1 µg/mL) to CoPc at 10 µg/mL in DMSO solution. The precipitated CoPc-GO hybrid materials were dropped onto double-sided carbon tape for SEM investigation. Before imaging, Au coating was performed for better conductivity and to avoid electron discharge onto materials due to the insulation properties of organics and graphene oxide, as well. Figure 5A and B show the partial agglomeration of GO within CoPc in DMSO solution is visible. By increasing GO concentration in DMSO, as CoPc remains constant, the initial 3D network formation was begun. Figure 5C and D show that the local 3D network formation is evident. The GO has formed a continuous porous network which improves the bonded GO's contiguity. Schematic representation of CoPc may give clues of bonding possibility of CoPc to GO from central and chains for oxygen bonding. The agglomerate formation possibility decreases by increased GO solution. A 3D network may be expected to form after reaction of -OH and -COOH groups by free oxygen of CoPc accompanied by DMSO solution to produce more resistant bonds by chain reaction as seen in CoPc schematic structure. DMSO is seen as an excellent solvent for CoPc and GO together due to free oxygen carriers and -OH/-COOH combinations. Besides, CoPc-GO interactions can also be called as noncovalent π–π interactions. These types of conjugation give rise to a better combination of CoPc and GO hybrid nanomaterial that is dissolvable in DMSO. This may also be due to the -OH and -COOH transfer to the solute to dissolve either one of ingredients to produce more sieve-like structure than Fig. 5A–B where low amount of GO cannot

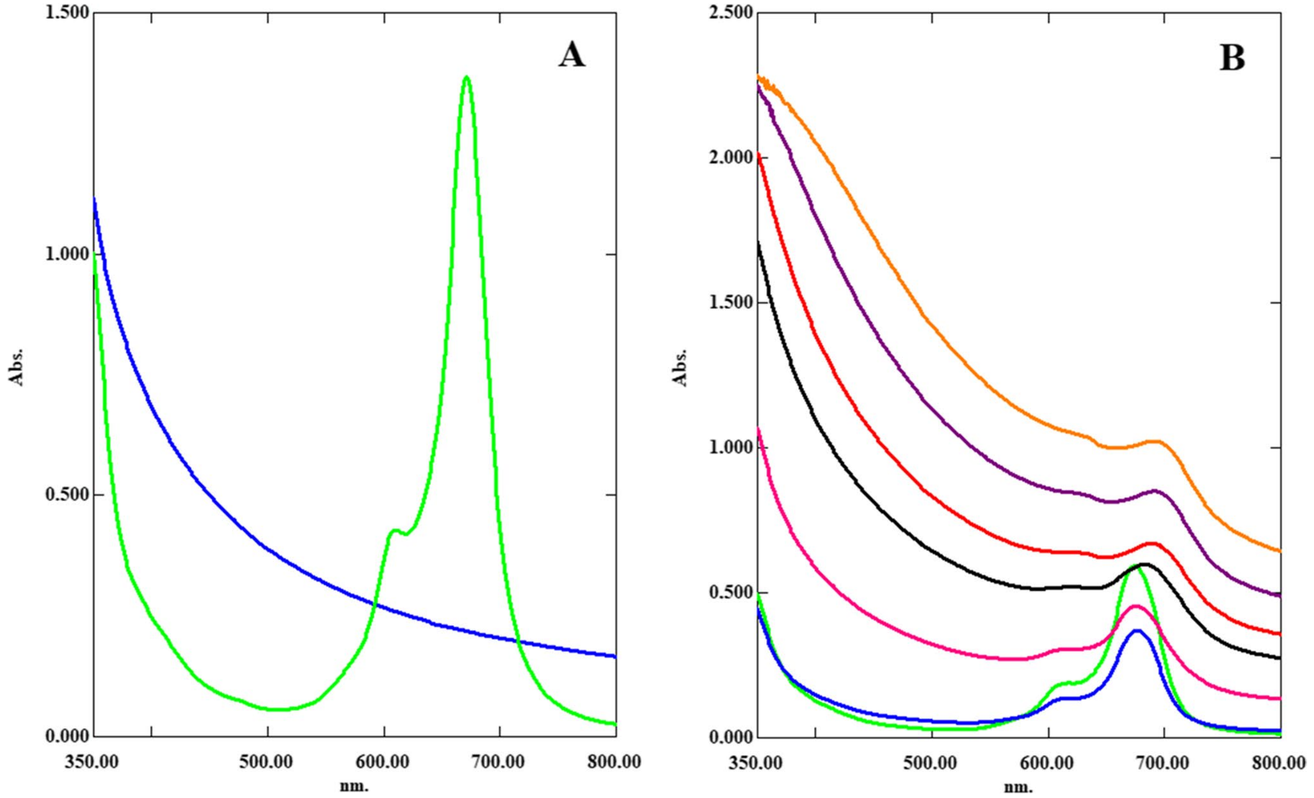

Fig. 2 **A** The UV–Vis spectra of CoPc (—) and GO (—). **B** The UV–Vis spectra of CoPc (10 μg/mL) in DMSO after addition of GO with various concentrations. [GO concentrations: 0.00005 μg/mL (—); 0.0005 μg/mL (—); 0.005 μg/mL (—); 0.05 μg/mL (—); 0.4 μg/mL (—); 0.7 μg/mL (—); 1 μg/mL (—)]

Fig. 3 Fluorescence spectra of DMSO solution of CoPc (10 μg/mL) against different concentrations of GO. [GO concentrations: 0.005 μg/mL; 0.05 μg/mL; 0.4 μg/mL; 1 μg/mL]. Excitation wavelength is 700 nm

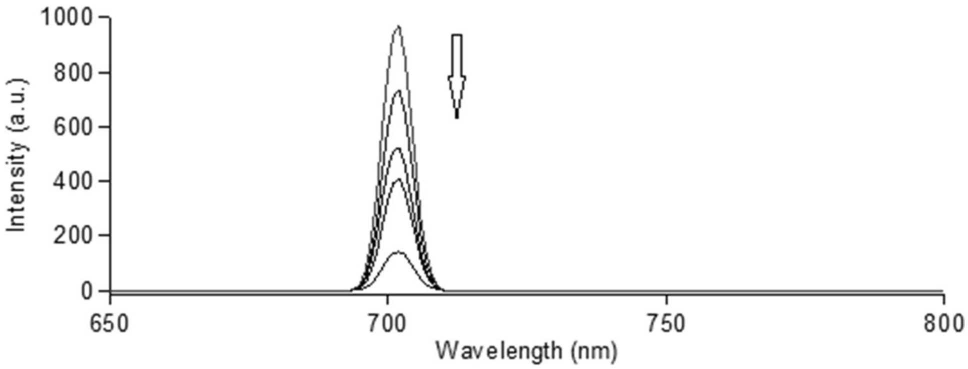

afford it. Since by increasing GO amount in solution, the UV spectra disappears, so the sieve-like structure can be said to increase and CoPc may dissolve or GO produces a 3D by -OH and -COOH chains together. There is a certain concentration that CoPc and GO combination makes changes in UV–Vis spectra; after that point, the peaks disappear unexpectedly without any sign of agglomeration that means the ingredients dissolved in DMSO instead of colloidal suspension formation of GO. Molecularly, CoPc dissolves while GO stands still as colloidal, but in this manner, π–π conjugation makes them a novel material as illustrated by absorption peaks.

SEM–EDX is seen in Fig. 6. The polygon shape indicates the formed 3D network of GO modified CoPc precipitated in DMSO. High-intensity C and O peaks are seen due to the carbon-rich organic structure; due to the low concentration, Co peaks are hardly seen. These results confirm CoPc-GO hybrid formation.

Examination of optical properties is very important as they provide information about the electronic structures and optical

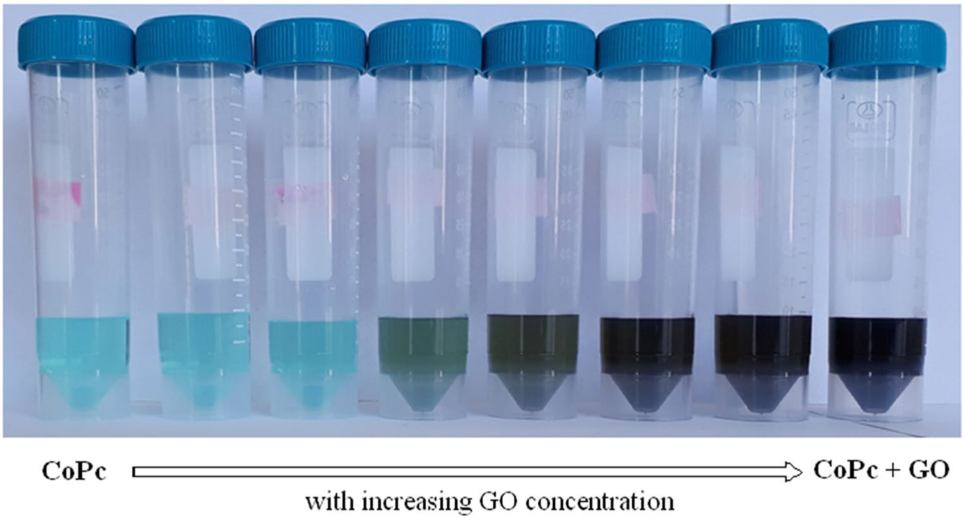

Fig. 4 Color change in CoPc-GO hybrids at varying concentrations of GO (concentration of GO increases from left to right)

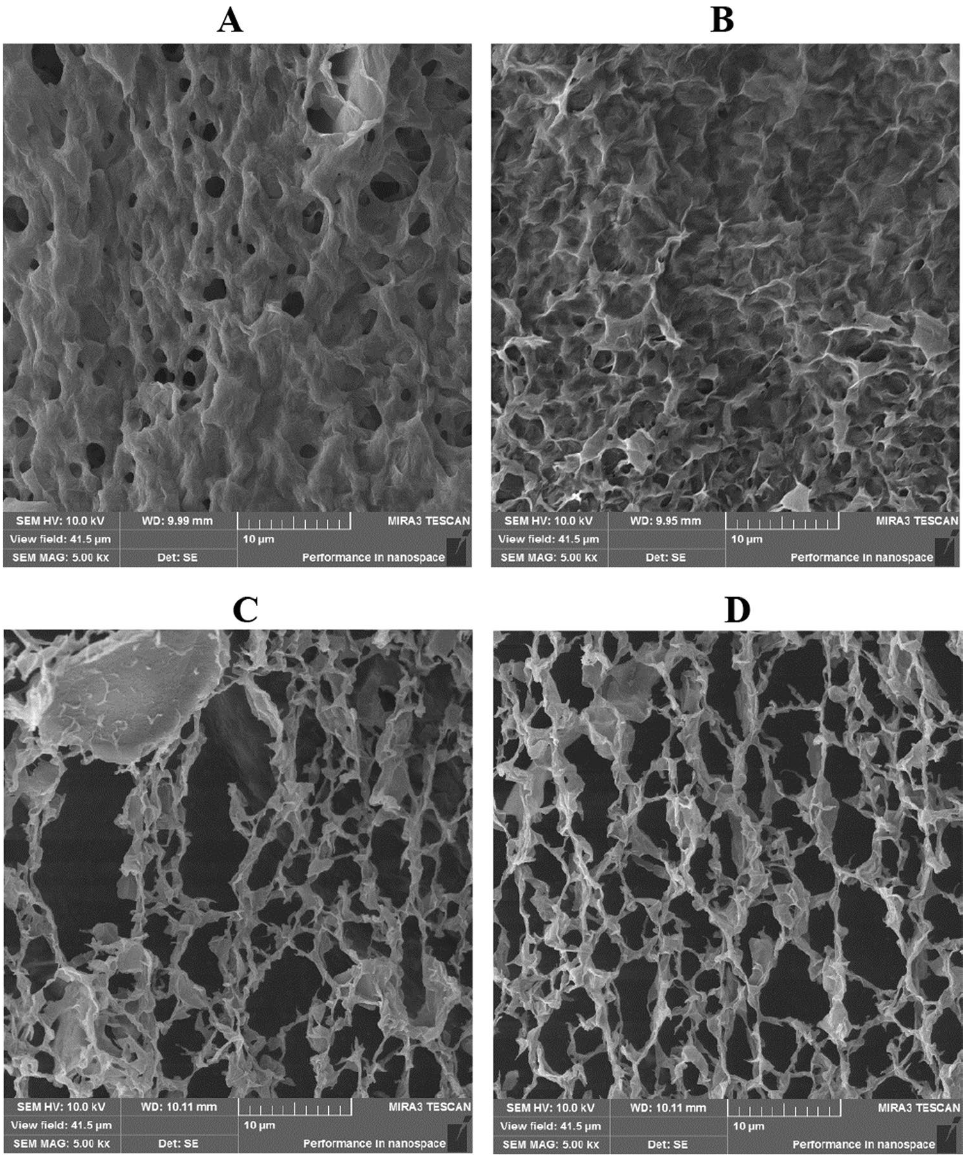

Fig. 5 SEM images of CoPc-GO nanomaterials, precipitated from DMSO solution [**A** CoPc-10 μg/mL; GO-0.0005 μg/mL; **B** CoPc-10 μg/mL; GO-0.005 μg/mL; **C** CoPc-10 μg/mL; GO-0.4 μg/mL; **D** CoPc-10 μg/mL; GO-1 μg/mL]

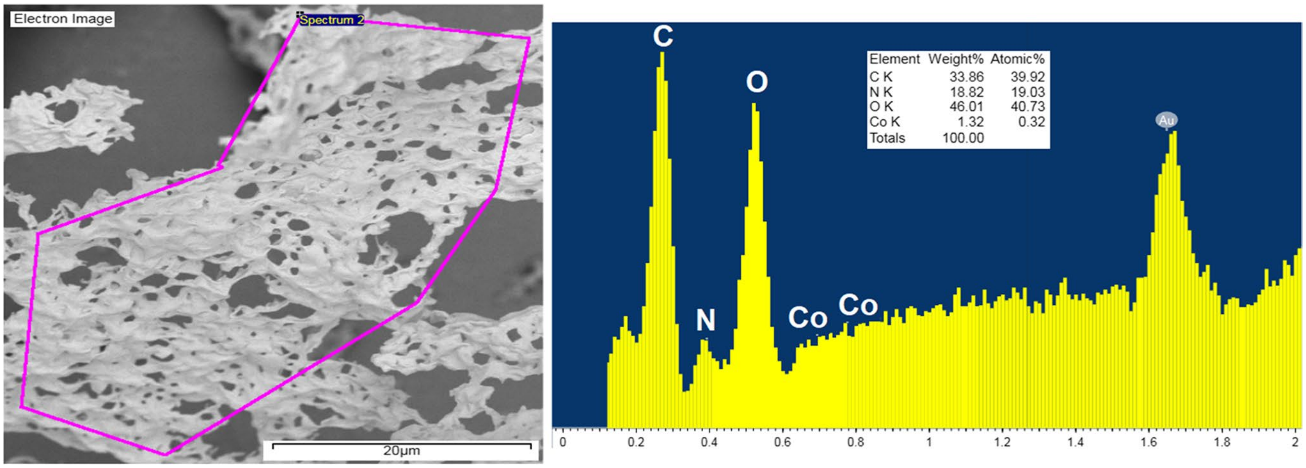

Element	Weight%	Atomic%
C K	33.86	39.92
N K	18.82	19.03
O K	46.01	40.73
Co K	1.32	0.32
Totals	100.00	

Fig. 6 SEM–EDX image of CoPc-GO hybrid (CoPc-10 µg/mL; GO-0.05 µg/mL) material precipitated from DMSO

transition types of a material [41]. The band gap is a vital parameter that determines the potential of semiconductors for photovoltaic applications. If the band gap of semiconductor materials falls into the visible region in the solar spectrum, it can be said that these materials can be used for photovoltaic application. When we look at the literature, there are studies in which phthalocyanine and its derivatives with a band gap between about 1.5 and 2.0 eV are effective in photovoltaic applications [42–45]. To determine the optical properties of the prepared nanomaterial, optical transmission and absorbance spectra of the thin film of the compound were taken at room temperature.

The optical band gap of CoPc-GO hybrid was determined from analysis of the absorption spectrum of the compound's thin film as described by the Tauc plot using the formula [46, 47].

$$\alpha h\nu = \alpha_o(h\nu - Eg)^n$$

where α is absorption coefficient, hν is the energy of the incident photons, and E_g is the value of the optical band gap energy (eV) corresponding to the transitions denoted by the n value. α_o is a constant that depends on the transition probability [46, 48, 49].

As seen in Fig. 7, extrapolating the Tauc plot to the abscissa gives the value of the optical band gap [46]. According to the graph, optical band gap of CoPc-GO hybrid was determined as 1.75 eV which makes these films attractive for photovoltaic applications.

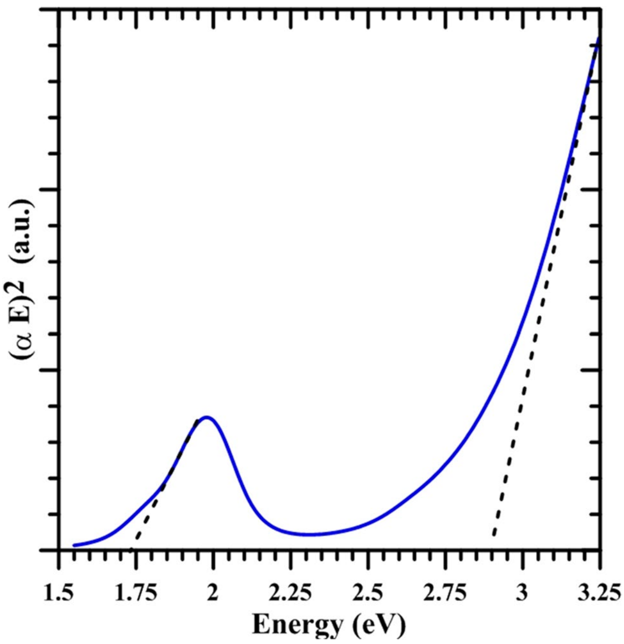

Fig. 7 Determination of the band gap of CoPc-GO hybrid thin film

Conclusions

In this study, a novel CoPc-GO hybrid nanomaterial was prepared by the self-assembly method, and it was observed that CoPc and GO derivatives were well coordinated. The formation of the novel CoPc-GO hybrid nanomaterial was characterized by UV–Vis, fluorescence spectroscopy, and SEM images. The measurements confirm that strong π–π interactions could be reached through in CoPc-GO hybrid formation. It was observed that the π–π stacking interactions shortly begin after mixing of CoPc and GO and are completed in 5 min of sonication. To the best of our knowledge, this is the first report to show that strong π–π interactions of CoPc and GO components could in fact be realized in such a short time. Also, the prepared CoPc-GO hybrid nanomaterial is stable even at room conditions and during dilution. Besides, the optical properties of the CoPc-GO hybrid were also examined in a UV–Vis spectrophotometer. The optical band gap of the nanomaterial was determined as 1.75 eV, suggesting. According to the optical band gap result, it can be said that the CoPc-GO hybrid has a potential to be used in optoelectronic applications.

Acknowledgements In this study, the laboratory facilities of the Advanced Technology Application and Research Center (CÜTAM) of Sivas Cumhuriyet University were used. The authors wish to thank Dr. Ali ÖZER for SEM images.

References

1. Chen, B., Liu, M., Zhang, L.M., Huang, J., Yao, J.L., Zhang, Z.J.: Polyethylenimine-functionalized graphene oxide as an efficient gene delivery vector. J. Mater. Chem. **21**, 7736–7741 (2011)
2. Yang, K., Wan, J.M., Zhang, S.A., Zhang, Y.J., Lee, S.T., Liu, Z.A.: *In vivo* pharmacokinetics, long-term biodistribution, and toxicology of PEGylated graphene in mice. ACS Nano. **5**, 516–522 (2011)
3. Zhang, Q., Li, W.W., Kong, T., Su, R.G., Li, N., Song, Q., Tang, M.L., Liu, L.W., Cheng, G.S.: Tailoring the interlayer interaction between doxorubicin-loaded graphene oxide nanosheetsby controlling the drug content. Carbon. **51**, 164–172 (2013)
4. Qin, X.C., Guo, Z.Y., Liu, Z.M., Zhang, W., Wan, M.M., Yang, B.W.: Folic acid-conjugated graphene oxide for cancer targeted chemo-photothermal therapy. J. Photochem. Photobiol. B. **120**, 156–162 (2013)
5. Eda, G., Chhowalla, M.: Chemically derived graphene oxide: towards large-area thin-film electronics and optoelectronics. Adv. Mater. **22**, 2392–2415 (2010)
6. Li, X.L., Zhang, G.Y., Bai, X.D., Sun, X.M., Wang, X.R., Wang, E.G., Dai, H.J.: Highly conducting graphene sheets and Langmuir-Blodgett films. Nat. Nanotechnol. **3**, 538–542 (2008)
7. Kim, F., Cote, L.J., Huang, J.X.: Graphene oxide: surface activity and two-dimensional assembly. Adv. Mater. **22**, 1954–1958 (2010)
8. Park, S., Ruoff, R.S.: Chemical methods for the production of graphenes. Nat. Nanotechnol. **4**, 217–224 (2009)
9. Bissessur, R., Scully, S.F.: Intercalation of solid polymer electrolytes into graphite oxide. Solid State Ionics. **178**, 877–882 (2007)
10. Paredes, J.I., Villar-Rodil, S., Martinez-Alonso, A., Tascon, J.M.D.: Graphene oxide dispersions in organic solvents. Langmuir. **24**, 10560–10564 (2008)
11. Compton, O.C., Nguyen, S.T.: Graphene oxide, highly reduced graphene oxide, and graphene: versatile building blocks for carbon-based materials. Small. **6**, 711–723 (2010)
12. Dong, L.F., Gari, R.R.S., Li, Z., Craig, M.M., Hou, S.F.: Graphene-supported platinum and platinum–ruthenium nanoparticles with high electrocatalytic activity for methanol and ethanol oxidation. Carbon. **48**, 781–787 (2010)
13. Chang, H.X., Lv, X.J., Zhang, H., Li, J.H.: Quantum dots sensitized graphene: ın situ growth and application in photoelectrochemical cells. Electrochem. Commun. **12**, 483–487 (2010)
14. Mohanty, N., Berry, V.: Graphene-based single-bacterium resolution biodevice and dna transistor: ınterfacing graphene derivatives with nanoscale and microscale biocomponents. Nano Lett. **8**, 4469–4476 (2008)
15. Paek, S.M., Yoo, E., Honma, I.: Enhanced cyclic performance and lithium storage capacity of SnO_2/graphene nanoporous electrodes with three-dimensionally delaminated flexible structure. Nano Lett. **9**, 72–75 (2009)
16. Liu, H., Gao, J., Xue, M.Q., Zhu, N., Zhang, M.N., Cao, T.B.: Processing of graphene for electrochemical application: noncovalently functionalize graphene sheets with water-soluble electroactive methylene green. Langmuir. **25**, 12006–12010 (2009)
17. Seger, B., Kamat, P.V.: Electrocatalytically active graphene-platinum nanocomposites. Role of 2-D carbon support in PEM fuel cells. J. Phys. Chem. C. **113**, 7990–7995 (2009)
18. Li, Y.M., Tang, L.H., Li, J.H.: Preparation and electrochemical performance for methanol oxidation of pt/graphene nanocomposites. Electrochem. Commun. **11**, 846–849 (2009)
19. Li, Y.J., Gao, W., Ci, L.J., Wang, C.M., Ajayan, P.M.: Catalytic performance of Pt nanoparticles on reduced graphene oxide for methanol electro-oxidation. Carbon. **48**, 1124–1130 (2010)
20. Yao, J., Shen, X.P., Wang, B., Liu, H.K., Wang, G.X.: In situ chemical synthesis of SnO_2–graphene nanocomposite as anode materials for lithium-ion batteries. Electrochem. Commun. **11**, 1849–1852 (2009)
21. Wang, Y., Lu, J., Tang, L.H., Chang, H.X., Li, J.H.: Graphene oxide amplified electrogenerated chemiluminescence of quantum dots and ıts selective sensing for glutathione from thiol-containing compounds. Anal. Chem. **81**, 9710–9715 (2009)
22. Dong, H.F., Gao, W.C., Yan, F., Ji, H.X., Ju, H.X.: Fluorescence resonance energy transfer between quantum dots and graphene oxide for sensing biomolecules. Anal. Chem. **82**, 5511–5517 (2010)
23. Wang, K., Liu, Q., Wu, X.Y., Guan, Q.M., Li, H.N.: Graphene enhanced electrochemiluminescence of CdS nanocrystal for H_2O_2 sensing. Talanta. **82**, 372–376 (2010)
24. Stankovich, S., Dikin, D.A., Compton, O.C., Dommett, G.H.B., Ruoff, R.S., Nguyen, S.T.: Systematic post-assembly modification of graphene oxide paper with primary alkylamines. Chem. Mater. **22**, 4153–4157 (2010)
25. Su, Q., Pang, S.P., Alijani, V., Li, C., Feng, X.L., Müllen, K.: Composites of graphene with large aromatic molecules. Adv. Mater. **21**, 3191–3195 (2009)
26. Tan, L., Zhou, K.G., Zhang, Y.H., Wang, H.X., Wang, X.D., Guo, Y.F., Zhang, H.L.: Nanomolar detection of dopamine in the presence of ascorbic acid at β-cyclodextrin/graphene nanocomposite platform. Electrochem. Commun. **12**, 557–560 (2010)
27. Stankovich, S., Piner, R.D., Chen, X.Q., Wu, N.Q., Nguyen, S.T., Ruoff, R.S.: Stable aqueous dispersions of graphitic nanoplatelets via the reduction of exfoliated graphite oxide in the presence of poly(sodium 4-styrenesulfonate). J. Mater. Chem. **16**, 155–158 (2006)
28. Zu, S.Z., Han, B.H.: Aqueous dispersion of graphene sheets stabilized by pluronic copolymers: formation of supramolecular hydrogel. J. Phys. Chem. C. **113**, 13651–13657 (2009)
29. Li, G.L., Liu, G., Li, M., Wan, D., Neoh, K.G., Kang, E.T.: Organo- and water-dispersible graphene oxide−polymer nanosheets for organic electronic memory and gold nanocomposites. J. Phys. Chem. C. **114**, 12742–12748 (2010)
30. Wang, Y., Li, Z.H., Hu, D.H., Lin, C.T., Li, J.H., Lin, Y.H.: Aptamer/graphene oxide nanocomplex for in situ molecular probing in living cells. J. Am. Chem. Soc. **132**, 9274–9276 (2010)
31. Liu, Y., Yu, D.S., Zeng, C., Miao, Z.C., Dai, L.M.: Biocompatible graphene oxide-based glucose biosensors. Langmuir. **26**, 6158–6160 (2010)
32. Liu, Z.F., Jiang, L.H., Galli, F., Nederlof, I., Olsthoorn, R.C.L., Lamers, G.E.M., Oosterkamp, T.H., Abrahams, J.P.: A Graphene

oxide˙streptavidin complex for biorecognition – towards affinity purification. Adv. Funct. Mater. **20**, 2857–2865 (2010)

33. Liu, Z.B., Xu, Y.F., Zhang, X.Y., Zhang, X.L., Chen, Y.S., Tian, J.G.: Porphyrin and fullerene covalently functionalized graphene hybrid materials with large nonlinear optical properties. J. Phys. Chem. B. **113**, 9681–9686 (2009)
34. Xu, Y.F., Liu, Z.B., Zhang, X.L., Wang, Y., Tian, J.G., Huang, Y., Ma, Y.F., Zhang, X.Y., Chen, Y.S.: A graphene hybrid material covalently functionalized with porphyrin: synthesis and optical limiting property. Adv. Mater. **21**, 1275–1279 (2009)
35. Karousis, N., Economopoulos, S.P., Sarantopoulou, E., Tagmatarchis, N.: Porphyrin counter anion in imidazolium-modified graphene-oxide. Carbon. **48**, 854–860 (2010)
36. Yang, H.F., Shan, C.S., Li, F.H., Han, D.X., Zhang, Q.X., Niu, L.: Covalent functionalization of polydisperse chemically-converted graphene sheets with amine-terminated ionic liquid. Chem. Commun. **26**, 3880–3882 (2009)
37. Lomeda, J.R., Doyle, C.D., Kosynkin, D.V., Hwang, W.F., Tour, J.M.: Diazonium functionalization of surfactant-wrapped chemically converted graphene sheets. J. Am. Chem. Soc. **130**, 16201–16206 (2008)
38. Söylemez, N., Yabaş, E., ŞahinBölükbaşı, S., Sülü, M.: Antioxidant activities of the new tetrasubstituted metal-free, Zn(II) and Co(II) monophthalocyanines. J. Porphyrins Phthalocyanines. **22**, 233–242 (2018)
39. Durmuş, M., Nyokong, T.: Synthesis and solvent effects on the electronic absorption and fluorescence spectral properties of substituted zinc phthalocyanines. Polyhedron. **26**, 2767–2776 (2007)
40. Kobayashi, N., Lever, A.B.: Cation- or solvent-ınduced supermolecular phthalocyanine formation: crown ether substituted phthalocyanines. J. Am. Chem. Soc. **109**, 7433–7441 (1987)
41. Cherian, R.C., Menon, C.S.: Preparation and characterization of thermally evaporated titanium phthalocyanine dichloride thin films. J. Phys. Chem. Solids. **69**, 2858–2863 (2008)
42. Senthilarasu, S., Velumani, S., Sathyamoorthy, R., Subbarayan, A., Ascencio, J.A., Canizal, G., Sebastian, P.J., Chavez, J.A., Perez, R.: Characterization of zinc phthalocyanine (ZnPc) for photovoltaic applications. Appl. Phys. A. **77**, 383–389 (2003)
43. Senthilarasu, S., Sathyamoorthy, R., Lee, S.H., Velumani, S.: Characterization of zinc-phthalocyanine–CdS composite thin films for photovoltaic applications. Vacuum. **84**, 1212–1215 (2010)
44. Timoumi, A., Wederni, M.A., Bouguila, N., Jamoussi, B., AL Turkestani, M.K., Chakroun, R., Al-Mur, B.: Electrical impedance spectroscopy study of unsubstituted palladium (II) phthalocyanine. Synt. Metal. **272**, 116659–116666 (2021)
45. Kannan, R.R., Nelson, P.I., Rajesh, S., Selvan, T.P., Mohan, A., Vidhya, B., Arivazhagan, D.N.: Curtailed recombination rate and fast carrier transport in ZnPc/GaAs/ZnPc stacked hybrid structure. Optic. Mater. **85**, 287–294 (2018)
46. Hamam, K.J., Alomari, M.I.: A study of the optical band gap of zinc phthalocyanine nanoparticles using UV-Vis spectroscopy and DFT function. Appl. Nanosci. **7**, 261–268 (2017)
47. El Nhass, M.M., Sollman, B.S., Metwally, B.S., Farid, A.M., Farag, A.A.M., El Shazly, A.A.: Optical properties of evaporated iron phthalocyanine (FePc) thin films. J. Opt. **30**, 121–129 (2001)
48. Kim, H.J., Kim, J.W., Lee, H.H., Lee, B., Kim, J.J.: Initial growth mode, nanostructure, and molecular stacking of a ZnPc:C60 bulk heterojunction. Adv. Funct. Mater. **22**, 4244–4248 (2012)
49. Mobtakeri, S., Akaltun, Y., Özer, A., Kılıç, M., Tüzemen, E.Ş, Gür, E.: Gallium oxide films deposition by RF magnetron sputtering; a detailed analysis on the effects of deposition pressure and sputtering power and annealing. Ceram. Int. **47**, 1721–1727 (2021)